Response of the nonlinear-nonstationary internal tide to the spring-neap cycle of the barotropic tide

Alfonso, Edwin[1] and Zachariah R. Hallock[2]

Abstract

Data from bottom-moored ADCPs deployed in the Mid-Atlantic Bight near 39.3 N, 72.7 W, offshore of the New Jersey Coast, are analyzed to reveal the dependence of semidiurnal baroclinic energy in shelf waters on changes in the barotropic forcing. The semidiurnal frequency band is defined between 1.76 -2.31 CPD. Baroclinic semidiurnal current speeds are mostly below 5 cm s^{-1}, but they can reach 9-18 cm s^{-1} during spring and neap tides. Strong semidiurnal baroclinic currents occur during neap barotropic tides. There is no coherence at the semidiurnal frequency between the barotropic and baroclinic tide at the shelf location. The kinetic energy of the semidiurnal internal tide usually represents less than 20% of the total baroclinic kinetic energy present in the ADCP record at this location. This percentage can increase from 40% up to 80% for brief periods (< 1 day). Maximum in PE energy and KE are 9 and 22 J m^{-3}, respectively. Hilbert Huang Transform (HHT) analysis and conventional empirical orthogonal function (EOF) analysis were combined into HEOF analysis. HEOF is applied to the data. This approach is effective for the analysis of nonstationary-nonlinear internal tides.

1 alfonso@nrlssc.navy.mil 228-688-4845, NRL Code 7332, Stennis Space Center, MS 39529

2 NRL Code 7332, Stennis Space Center, MS 39529

To see posters http://www7320.nrlssc.navy.mil/pubs/

Figure 1

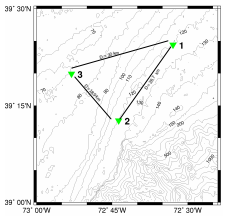

Figure 2

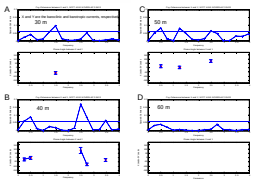

Figure 11

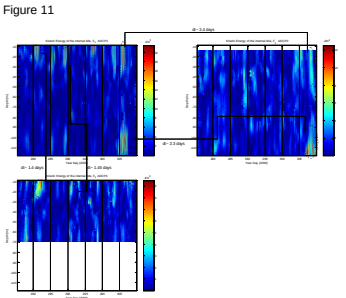

Methodology

Figure 1 shows the location of the ADCP moorings. The raw ADCP data must be carefully process to obtain a signal that consists primarily of baroclinic tidal energy (Figure 3). This signal (matrix X) will be the original input into HEOF analysis. Hilbert-Huang Transform (HHT) and conventional empirical orthogonal function (EOF) analysis are combined to form HEOF analysis. HEOF analysis is based on modal decompositions of a covariance matrix calculated from the Empirical Mode Decomposition (EMD) of the original series. We present two implementation approaches of HEOF : the first one consists in EMD, EOF, Hilbert Spectrum Analysis (HSA) and the second one in EMD, Hilbert Transform, and EOF, in that respective order (Figure 4). EMD analysis (Huang et al. 1998) can isolate the nonstationary nonlinear semidiurnal internal tide (F1, Figure 5). Kinetic energy , KE=0.5 ? (u^2+v^2), was calculated from F_1: u,v. Potential energy was derived from the KE by means of the ratio PE/KE = (? ^{2}-f^2) / (? ^{2}+f^2)= 0.4; (Gill, 1992).

Figure 3

Steps to prepare the signal for HEOF analysis

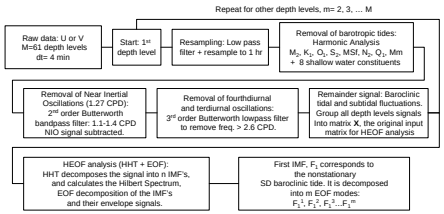

Figure 4

Two approaches for HEOF analysis

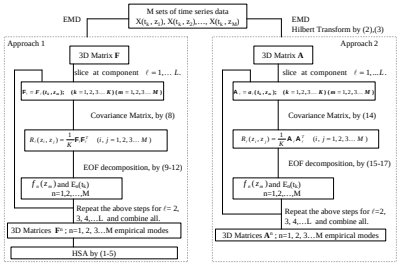

Figure 5

IMF sifting of u (t_k , z) z=30 m, k = 1,2,3…K ; CE(100,5)

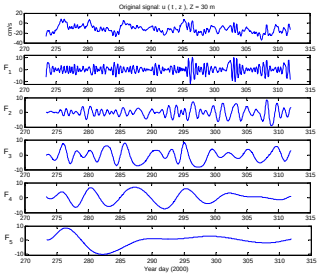

Table 1

First IMF ℓ=1	1st Approach F_ℓ^n	2nd Approach A_ℓ^n
Mode number n	Explained Variance	Explained Variance
1	55.91%	49.14%
2	15.87%	13.34%
3	10.29%	11.72%
4	6.48%	7.45%
5	2.63%	4.28%
6	2.34%	2.43%
Subtotal	93.52%	88.36%

Results

Figure 2A-D shows that there is not significant coherence between the baroclinic and baroclinic tide at semidiurnal frequencies (2 CPD). The following results (except Figure 11) correspond to the analysis of ADCP3 data (station 3, Figure 1). For brevity, we limited to show component (east-west) of u in Figures 5-7 and 10. Figure 6A-D shows the results of the first approach of HEOF. It shows a colored code image of the east-west component of the SD baroclinic tide $\mathbf{F_1}$ at ADCP3 and its first three EOF modes: F_1^1, F_1^2, F_1^3. The amount of variance explained by each mode is shown in Table 1. Results of the second approach are shown in Figure 7A-D; the modulation signal of the baroclinic tide, A_1 , and its corresponding modes: A_1^1, A_1^2, A_1^3.. Kinetic and potential energies were calculated for F_1 and its corresponding modes (Figure 8-9). The ratio between the KE of F_1 and the total baroclinic energy (including inertial freq.) show that the baroclinic tide can become a major part on brief periods (hours) but usually represents less than 20 % of the total energy. Figure 11 shows the Kinetic Energy of F1 at each of the moorings: ADCP1, ADCP2, ADCP3. More energetic internal tides are observed in ADCP1. Focusing our attention on particular strong events (dashed ellipses) its obvious than a significant time lag of the internal tide energy can occur in relatively short distances. Comparing the previous results with the barotropic spring-neap cycle (Figure 12), it is evident that equally energetic baroclinic tides can occur during barotropic neap tides as during spring tides.

Figure 6

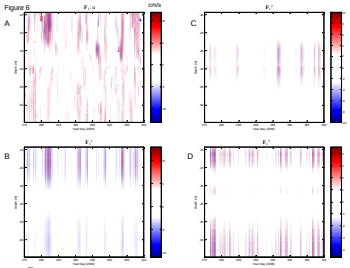

Figure 8

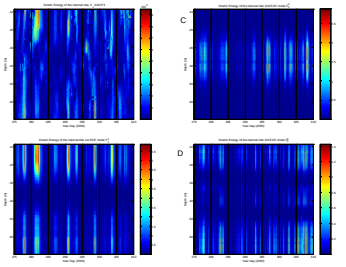

Figure 10

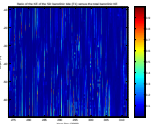

Figure 7

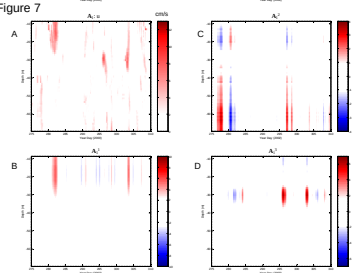

Figure 9

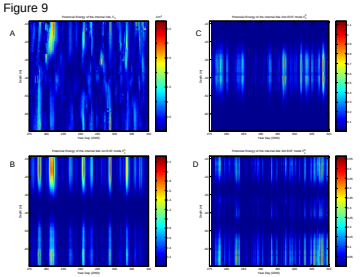

Figure 12

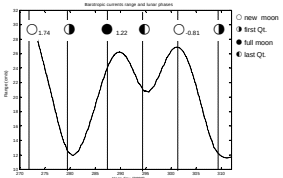

Acknowledgments

This work was supported by the American Society for Engineering Education (ASEE), the Office of Naval Research and the Naval Research Laboratory, Stennis Space Center.